Prediction of Human Eye Fixations using Symmetry

Gert Kootstra (G.Kootstra@ai.rug.nl)
Lambert R.B. Schomaker (L.Schomaker@ai.rug.nl)
Artificial Intelligence, University of Groningen
Nijenborgh 9, 9747 AG Groningen, the Netherlands

Abstract

Humans are very sensitive to symmetry in visual patterns. Reaction time experiments show that symmetry is detected and recognized very rapidly. This suggests that symmetry is a highly salient feature. Existing computational models of saliency, however, have mainly focused on contrast as a measure of saliency. In this paper, we discuss local symmetry as a measure of saliency. We propose a number of symmetry models and perform an eye-tracking study with human participants viewing photographic images to test the models. The performance of our symmetry models is compared with the contrast-saliency model of Itti, Koch and Niebur (1998). The results show that the symmetry models better match the human data than the contrast model, which indicates that symmetry can be regarded as a salient feature.

Keywords: visual perception; overt visual attention; symmetry; saliency; saliency models

Introduction

While viewing the world, humans constantly make eye movements to fixate on interesting parts of the visual field. In this way, the relevant information can be viewed with high resolution, while irrelevant information can be ignored. The process of focusing attention by making an eye movement is called *overt visual attention*. The eye movements are influenced both top-down, emerging for instance from past experiences, personal interests, and the task, as well as bottom-up, purely from the stimulus. In the current research, we are interested in the stimulus-driven influences on eye movements, without semantic control. What in the stimulus causes our eyes to move to a certain location? What causes certain parts of the visual field to catch attention? More specifically, we investigate how well the locations of eye fixations can be predicted on the basis of local symmetry.

Most current models of visual attention base their predictions on contrast in the image. The model of Itti and Koch (Itti & Koch, 2001; Itti, Koch, & Niebur, 1998), for instance, is based on contrasts in luminance, color and orientation. Their saliency model is an implementation of the feature integration theory of human visual search (Treisman & Gelade, 1980). The saliency model of Itti and Koch has been compared to human eye fixations by Parkhurst, Law and Niebur (2002). They tested the model on photographic images and showed that it matches the human fixation points significantly better than expected by chance. Ouerhani, von Wartburg, Hügli and Müri (2004) also found a positive correlation between the model and human fixations.

Also other saliency models, like the model of Le Meur, Le Callet, Barba and Thoreau (2006) are based on contrast calculations. They found a positive correlation between their model and human data that was slightly higher than the per-
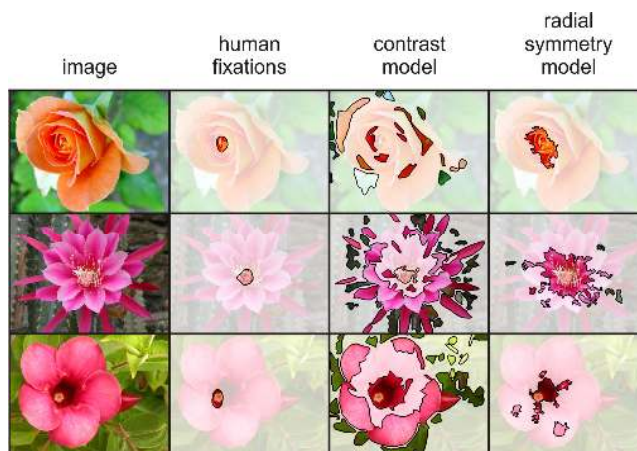

Figure 1: Examples of images containing symmetrical forms. The second column shows the human fixation density maps, the third shows the contrast-saliency maps, and the last shows the symmetry-saliency maps. The preference of humans to fixate on the center of symmetry is correctly reproduced by the symmetry model. The bright regions are the parts of the maps above 50% of its maximum value.

formance of Itti and Koch's model. Privitera and Stark (2000) investigated a set of simpler saliency operators including other features than contrast. The operators were also found to predict human fixation points to some extent. It must be noted that Privitera and Stark also used a simple symmetry operator that weakly resembled the human data.

However, even though most existing models are based on contrast, Figure 1 shows that humans have a clear preference to fixate on the center of symmetry for some images (second column). This can not be explained using contrast. Instead, the contrast model gives high response at the boundaries, where the flowers contrast with the background (third column). This apparent deficiency in current vision models was the motivation for the present study.

The human response, shown in Figure 1, suggests that humans pay attention to symmetrical forms. In this paper we will investigate if eye fixations can be predicted on the basis of local symmetry. As can be appreciated in the last column in Figure 1, our symmetry saliency model does predict fixations in accordance with the human data. We will show that this is not only valid for images that contain explicit symmetrical forms like those in Figure 1, but more generally in complex photographic images with different types of content.

Symmetry is a prominent visual feature in our daily environments. Many living organisms, for instance, have clear left-right symmetry in their bodies. This symmetry is even
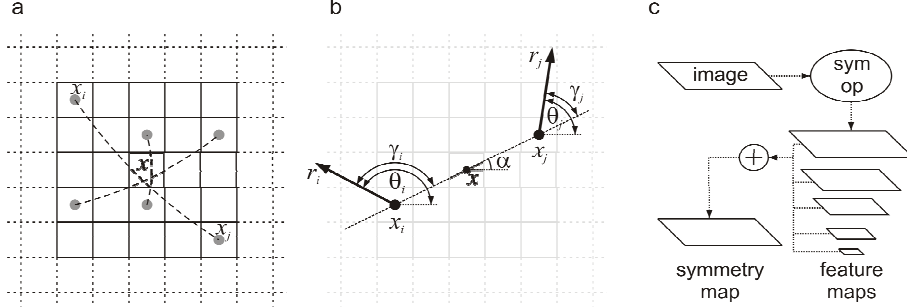
Figure 2: The basis of our symmetry models. (a) gives three examples of pixel pairs whose gradients are compared by the symmetry operator. The geometry of the contribution of a pixel pair is shown in (b) and further explained in the text. (c) gives an overview of the multi scale setup of the symmetry models.

an indication of the fitness of the individual. For instance, manipulated images of faces with enhanced symmetry are judged more attractive than the original faces (Grammer & Thornhill, 1994). Also in art, symmetry is usually preferred over asymmetry (Tyler, 2000). According to Gestalt psychologists symmetry improves the *figural goodness* (Palmer, 1991). Because symmetry is so prominent, it is likely that it plays a role in the visual system.

It is also known that humans are sensitive to symmetry. Symmetrical patterns are detected very rapidly, especially when having multiple axes of symmetry (Palmer & Hemenway, 1978). Also recognition performances increase with symmetrical patterns (Royer, 1981). The increase in performance might be explained by the intrinsic redundancy present in symmetrical forms, which gives rise to simpler representations (Barlow & Reeves, 1979). Humans furthermore have the tendency to interpret symmetrical regions as figure, and asymmetrical regions as background (Driver, Baylis, & Rafal, 1992).

Symmetry also influences eye movements. Fixations on symmetrical forms are concentrated at the center (Richards & Kaufman, 1969) of the form, or at the crossing points of the symmetry axes (Kaufman & Richards, 1969). For images with a single symmetry axis, the fixations are concentrated along this axis, whereas the fixations are more spread out for non-symmetrical images (Locher & Nodine, 1987). These studies, however, use simple stimuli with only one symmetrical pattern presented.

In this paper, we investigate the role of local symmetry on overt visual attention in complex photographic scenes, and compare it to the role of contrast. We propose extended symmetry-saliency models, and compare their performances with the contrast saliency model of Itti and Koch, henceforth referred to as the *contrast model*. We show that the symmetry models correspondd significantly better with the human eye fixations.

Methods

To investigate the role of symmetry in visual attention, we developed a number of symmetry-saliency models and compared them with human eye tracking data. To establish a point of reference, the contrast-saliency model of Itti *et al.*

(Itti *et al.*, 1998) is also compared with the human data. In this section, the developed symmetry-saliency models are explained, followed by a description of the eye-tracking studies and the method to compare the models with the human data.

Symmetry operators

Our models are based on the isotropic symmetry and radial symmetry operator of Reisfeld, Wolfson and Yeshurun (1995), and on the color symmetry operator of Heidemann (2004). We extended the operators to multi-scale symmetry-saliency models.

The *isotropic symmetry operator* (Reisfeld *et al.*, 1995) calculates the amount of symmetry at a given position, x, based upon gradients of the intensity in surrounding pixels. This is done by comparing pairs of pixels i and j at positions x_i and x_j, where $x = (x_i + x_j)/2$ (see Figure 2a). Every pixel pair contributes to the local symmetry by

$$c(i, j) = d(i, j, \sigma) \cdot p(i, j) \cdot m_i \cdot m_j \qquad (1)$$

Where m_i is the magnitude of the gradient at point i, $d(i, j, \sigma)$ is a Gaussian weighting function on the distance between the two pixels with standard deviation σ, and the symmetry measurement $p(i, j)$ is calculated by

$$p(i, j) = \left(1 - \cos(\gamma_i + \gamma_j)\right) \cdot \left(1 - \cos(\gamma_i - \gamma_j)\right) \qquad (2)$$

Where $\gamma_i = \theta_i - \alpha$ is the angle between the direction of the gradient angle θ_i and the angle α of the line between p_i and p_i (see Figure 2b). The first term in equation (2) has a maximum value when $\gamma_i + \gamma_j = \pi$, which is true for gradients that are mirror symmetric with respect to p. Using only this term would result in high values for points on a straight edge, which are not considered symmetrical. To avoid this problem, the second term demotes pixel pairs with similar gradient orientation. In this way, the contributions of all pixel pairs, $\Gamma(p)$, within the radius, r, are summed up to give the isotropic symmetry value for p:

$$\mathcal{M}^{\text{iso}}(x, y) = \sum_{(i, j) \in \Gamma(p)} c(i, j) \qquad (3)$$

To make the symmetry operator more sensitive to symmetrical patterns with multiple axes of symmetry, Reisfeld

Figure 3: Examples of images used, one for each category: flowers, animals, street scenes, buildings and nature.

et al. (1995) developed the *radial symmetry operator* as an extension of the isotropic symmetry operator. First, the orientations of the contribution of the pixel pairs are calculated by $\varphi(i, j) = (\theta_i + \theta_j)/2$. Next, the symmetry orientation is determined as $\phi(p) = \varphi(i, j)$ for (i, j) that give the highest contribution $c(i, j)$. This value is then used to promote the contributions of pixels pairs with dissimilar orientations:

$$\mathcal{M}^{\text{rad}} = \sum\nolimits_{(i,j) \in \Gamma(p)} c(i, j) \cdot \sin^2\left(\varphi(i, j) - \phi(p)\right) \qquad (4)$$

The two symmetry operators mentioned above work on intensity values only. Since some color transitions are not detectable in gray-valued images, Heidemann (2004) adapted the isotropic symmetry operator to the *color symmetry operator*. This operator uses three color channels, red, green and blue. Equation (3) is adapted so that not only the gradients of pixels in one channel, but also between different channels are compared:

$$\mathcal{M}^{\text{col}}(x, y) = \sum_{(i,j) \in \Gamma} \sum_{(k_i, k_j) \in K} c(i, j, k_i, k_j) \qquad (5)$$

where K contains all combinations of color channels, and $c(i, j, k_i, k_j)$ is the symmetry contribution calculated by comparing pixel i in color channel k_i with pixel j in color channel k_j. Furthermore, equation (2) is altered to:

$$p(i, j) = \cos^2(\gamma_i + \gamma_j) \cdot \cos^2(\gamma_i) \cdot \cos(\gamma_j) \qquad (6)$$

so that the function gives the same result for gradients that are rotated 180°. The second term keeps the same functionality as the second term in equation (2).

Symmetry-saliency models

The human visual system is thought to process information on multiple spatial scales. We therefore adapted the above described operators to multi-scale saliency models, similarly to (Itti *et al.*, 1998).

The process to calculate the symmetry maps is depicted in Figure 2c. First, five spatial scales of the input image are created by progressively applying a Gaussian filter followed by a downscaling of the image by a factor of two. The different scales are then processed to symmetry feature maps using the symmetry operators as discussed in the previous section, where we use $r = 24$ and $\sigma = 36$. Next, the five feature maps are normalized using the normalization operator, *N*, used in (Itti *et al.*, 1998). This normalization consists first of scaling the feature map values to the range [0..1], and then multiplying the feature map with $(1 - \bar{m})^2$, where $\bar{m}$ is the average value of all local maxima in the map. This normalization promotes feature maps that contain a small number of symmetrical patterns that really stand out, as opposed to feature maps that contain many patterns with simi-

lar symmetry values. Finally, the feature maps are combined into a symmetry saliency map by resizing all feature maps to the same size and summing them.

$$\mathcal{S} = \overset{4}{\underset{s=0}{\oplus}} N(\mathcal{M}_s) \qquad (7)$$

Where $\oplus$ is the summation operator that resizes all parts to the same size, and $\mathcal{M}_s$ is the symmetry feature map at scale s. This procedure results in three symmetry saliency maps: $\mathcal{S}^{\text{iso}}$ for isotropic symmetry, $\mathcal{S}^{\text{rad}}$ for patterns with multiple symmetry axes, and $\mathcal{S}^{\text{col}}$ which uses color information.

Eye-tracking experiment

We recorded human fixation data in an eye-tracking experiment using the Eyelink head-mounted eye-tracking system (SR research). Fixation locations were extracted using the accompanied software. The images were displayed full-screen with a resolution of 1024 by 768 pixels on an 18'' CRT monitor of 36 by 27 cm at a distance of 70 cm from the participants. The visual angle was approximately 29º horizontally by 22º vertically. Before the experiment, the eye tracker was calibrated using the Eyelink software. The calibration was verified prior to each session, and recalibrated when needed.

Since we are interested in the bottom-up components of visual attention, the participants were asked to freely view the images. We did not give them a task, since that would give a strong bias on the eye movements. Our approach is similar to (Kootstra, Nederveen, & De Boer, 2008; Le Meur *et al.*, 2006; Parkhurst & Niebur, 2003).

31 students (15 female) of the University of Groningen took part for course credits. The age of participants ranged from 17 to 32. All had normal or corrected-to-normal vision. In the experiment, 99 images in five different categories were presented, 19 images of natural symmetrical objects, 12 images of animals in a natural setting, 12 images of street scenes, 16 images of buildings, and 40 images of natural environments (see Figure 3). Only the images in the first category were selected for their symmetrical content. The other categories represent a wide variety of images, containing natural and cultural scenes, with organic and rectilinear shapes. All these images were taken from the McGill calibrated colour image database (Olmos & Kingdom, 2004). The experiment was split up into sessions of approximately 5 minutes. Between the sessions, the experimenter had a short relaxing conversation with the participants, in order to get them motivated and focused for the next session. Before starting a new session, the calibration of the eye tracker was verified. After each presented images, drift was measured and corrected if needed using the Eye-
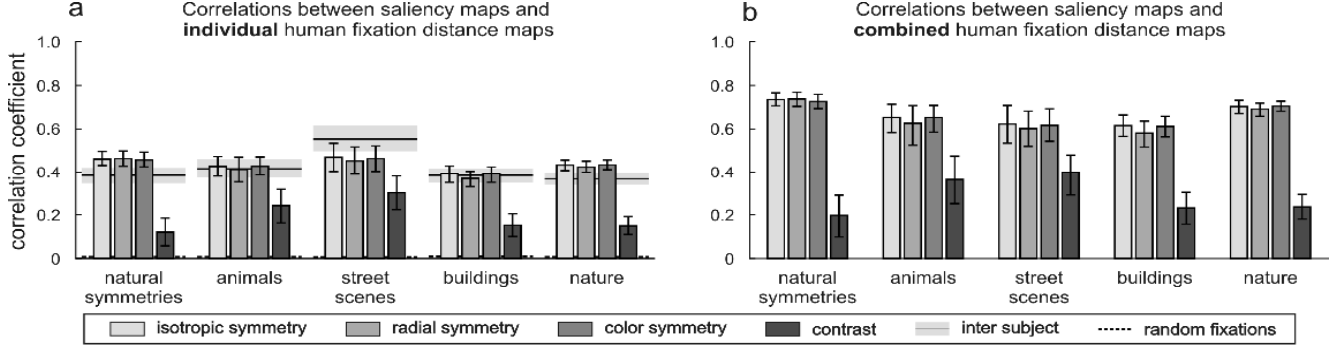
Figure 4: (a) The correlations results with the individual fixation-distance maps. The groups give the results for the different image categories. The error bars are the 95% confidence intervals. The horizontal gray bars with the solid line show the mean and 95% confidence interval of the inter-participant correlation. The dashed lines show the correlation of the human data with random fixations (close to zero). (b) The correlation results with the combined fixation-distance maps, representing the consensus among the participants. The patterns in both plots are similar, but with higher correlations for the later.

link software. The participants could decide when to continue and were allowed to take a short break.

Analysis methods

To compare the saliency models with the human data, we use two methods. A *correlation method* similar to that used in (Le Meur *et al.*, 2006; Ouerhani *et al.*, 2004), and a *fixation-saliency method*, similar to that used in (Parkhurst *et al.*, 2002).

The correlation method correlates the saliency maps with *fixation-distance maps* calculated from the human fixation data. For every single trial of every participant, the fixation-distance map is calculated using the inverse *distance transform*. The distance transform of the human data gives the distance to the nearest human fixation for all the pixels in the image. At the points of fixation, the values are thus zero, and they increase linearly for pixels farther from the fixations. We then take the inverse of the distance transformation. This is done by subtracting all distance values from the maximum distance value. The inverse distance map, which we call the *fixation-distance map*, therefore contains high values close to the fixation points, and lower values at points far from the fixations, and can be seen as a probability distribution for fixations. This is slightly different from the approach in (Kootstra *et al.*, 2008; Le Meur *et al.*, 2006; Ouerhani *et al.*, 2004), where a fixation density map is calculated using Gaussian kernels. Our method puts emphasis on the location of fixations, rather than on their density. Moreover, our method is parameter free, i.e., there is no width of the kernel to be set.

The value of the comparison between the saliency map and the fixation-distance map is then given by the correlation coefficient, ρ:

$$\rho = \frac{\sum_{x,y}\left(\left(\mathcal{F}(x,y)-\mu_{\mathcal{F}}\right)\cdot\left(\mathcal{S}(x,y)-\mu_{\mathcal{S}}\right)\right)}{\sqrt{\sigma_{\mathcal{F}}^2\cdot\sigma_{\mathcal{S}}^2}} \qquad (8)$$

where $\mathcal{F}$ is the fixation-distance map, $\mathcal{S}$ is the saliency map and μ and σ^2 are respectively the mean and the variance of the values in these maps. The correlation coefficient has a value between -1 and 1. A ρ of 0 means that there is no correlation between the two maps, which is true when correlating with random fixation-distance maps. Values for ρ close to zero indicate that a model is a poor predictor of human fixation locations. Positive correlations show that there is similar structure in the saliency map and the human fixation map.

This method calculates the correlation for individual participants. However, the photographic images viewed by the participants are highly complex stimuli that generate many fixations, with substantial variation among participants. Because of this variation, the correlations of individual fixation-distance maps with the saliency maps will be low. However, some of the fixations are shared by all participants. To see how well our models predict this consensus among participants, we also calculate the correlation coefficient for the *combined fixation-distance maps*, $\mathcal{F}_{tot} = \sum_{i=1}^{N}\mathcal{F}_i$, using equation (8).

The second comparison method, the fixation-saliency method, measures the saliency value, according to the saliency models, at the points of human fixation relative to the average saliency value at a large number of randomly chosen locations:

$$\lambda_i = s(f_i)\Big/\sum_{j=1}^{1000}s(\text{rnd}) \qquad (9)$$

Where λ_i is the fixation-saliency value for the *i*th fixation, f_i is the *i*th human fixation location and rnd is a randomly determined location in the image, excluding the borders. $s(p)$ is the average saliency value in a patch of the saliency map, $\mathcal{S}$, centered at point p and with a radius of 28 pixels. If $\lambda_i > 1$, the saliency at human fixation points is higher than in the rest of the image, meaning that the given saliency model has predictive powers.

Results

In Figure 4a, the results of the correlation between the individual fixation-distance maps and the saliency methods are
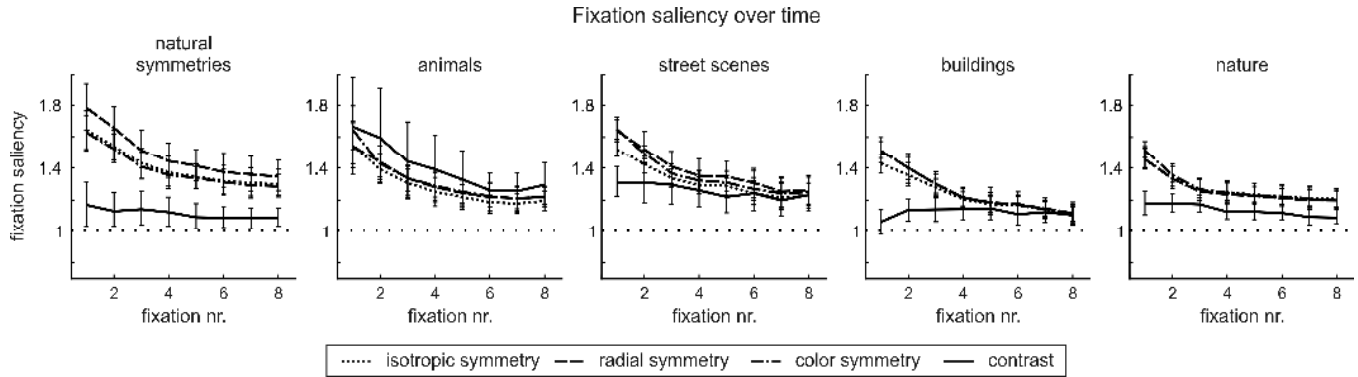
Fixation saliency over time

Figure 5: The plots give the saliency values at the fixation points relative to the average saliency in the image for the five image categories. Time, measured in fixation units is plotted on the horizontal axis. The fixation-saliency values for the three symmetry models and the contrast model of Itti and Koch are shown. The horizontal dotted line gives the expected value when fixations are random (i.e., 1.0), and the error bars are the 95% confidence intervals.

shown. The five groups of bars contain the results for the different image categories. Within each group, the bars show the mean correlation coefficients for the saliency models. The error bars give the 95% confidence intervals on the mean. The scores of the saliency methods are plotted along with the inter-participant correlation, and the correlation of the human data with random fixations. The first is depicted by the horizontal gray bar with a solid mid-line, giving the mean and 95% confidence interval. The correlation with random fixations is depicted by the horizontal dashed line, which is, as expected, virtually zero for all categories. All means and confidence intervals are calculated using multi-level bootstrapping. Significant differences can be appreciated by looking at the 95% confidence intervals.

The inter-participant correlation is calculated for every image by correlating the fixation-distance maps of the participants with those of all other participants, resulting in a similarity measure among participants. The plot shows that there is variability among the participants. The saliency methods are also faced with this variability, which pulls down the correlation values. The inter-participant correlation can therefore be used to put the scores of the saliency methods into perspective. The correlation scores of the models can be higher when the variation is high.

Looking at the bars and the 95% confidence intervals in Figure 4a, it can be appreciated that the performance of the three symmetry models is significantly higher than that of the contrast model. This is not only true for the natural symmetry images containing explicit symmetrical forms, also for the other categories the symmetry models significantly outperform the contrast model. For all categories, the performance of the symmetry models is in the same range as the inter-participant score. Among the three symmetry models, there is no significant difference in performance.

The values in Figure 4a are relatively low, caused by the variability among participants. Figure 4b shows the results of the comparison of the human data with the combined fixation-distance maps. This gives the similarity between the saliency models and the consensus among participants.

Figure 4b shows a very good match between the symmetry models and the human data for all images, suggesting that the common fixations of the participants are captured. The difference with the contrast-saliency model is significant.

Figure 5 shows the fixation-saliency values as a function of the fixation number. For all image categories, the symmetry models have high values for the early fixations, and gradually dropping values for later fixations. This shows that humans first fixate on highly symmetrical parts of the images. The fixation-saliency scores for the contrast model, on the other hand, are more or less constant over time, except for the animal category. For the images containing natural symmetries, the difference with the contrast saliency model is highly significant for all fixations. But also for most other categories, the symmetry models score better, especially at the first few fixations. For the street-scene, the building, and the nature categories, symmetry at early fixations is significantly higher than contrast. For later fixations, the difference is less apparent, but still in favor of the symmetry models, and significant for the nature category. For the animal category, we see a different picture. There, the symmetry and contrast model do not significantly differ, with higher scores for the contrast model. Furthermore, the contrast values are not constant for this category, but drop over time. This difference can be explained by the fact that the animal images contain objects (the animals) that are highly distinguishable from their, often, more or less uniform and blurry background. In contrast, the fore- and background in the other categories are less distinct, and more cluttered.

Discussion

We proposed three symmetry saliency models to investigate the role of local symmetry in guiding eye fixations. To test the performance of the models, we conducted an eye-tracking study, and evaluated the prediction of the models with the human data. We used the contrast saliency model of Itti and Koch (Itti *et al.*, 1998) to compare our results.

The results clearly show that human eye fixations can be significantly better predicted with our symmetry models

than with the contrast model. Our models show a significantly better correlation with the human data, comparable with the inter-participant correlation, for the individual participants. Particularly when we look at the combined fixation-distance maps, we see a very good match, showing that the proposed models predict the general consensus. The proposed models are general models in the sense that they do not only perform well on the images containing natural symmetrical objects, but also on images that are not selected for their symmetrical content. Moreover, the fixation-saliency analysis shows that especially early fixations are on highly symmetrical content, suggesting that symmetry is a good predictor of involuntary eye fixations, which are presumably more bottom-up controlled.

A possible explanation that symmetry is a good predictor of eye fixations is that eye movements are object oriented. Symmetry is known to play a role in figure-ground segregation (Driver *et al.*, 1992). Local symmetry can therefore serve as a bottom-up cue for the presence of an object in the image, which is then further inspected by making a fixation.

We expected the radial symmetry model to outperform the isotropic symmetry model since psychophysical studies showed that humans are more sensitive to forms with multiple symmetry axes (Palmer & Hemenway, 1978). However, this did not result in a significant increase in performance. This can be explained by the fact that the isotropic model already gives a stronger response to patterns with multiple symmetry axes. Also color does not improve the model.

Contrast obviously also plays a role in bottom-up attention. In future research, we would like to study the combination of contrast and symmetry for the prediction of fixations.

To conclude, the symmetry models that we developed are good predictors of visual attention, suggesting that humans pay attention to symmetry.

References

Barlow, H. B., & Reeves, B. C. (1979). The Versatility and Absolute Efficiency of Detecting Mirror Symmetry in Random Dot Displays. *Vision Research, 19*, 783-793.

Driver, J., Baylis, G. C., & Rafal, R. D. (1992). Preserved figure-ground segregation and symmetry perception in visual neglect. *Nature, 360*, 73 - 75.

Grammer, K., & Thornhill, R. (1994). Human (Home sapiens) Facial Attractiveness and Sexual Selection: The Role of Symmetry and Averageness. *Journal of Comparative Psychology, 108*(3), 233-242.

Heidemann, G. (2004). Focus-of-Attention from Local Color Symmetries. *IEEE Transactions on Pattern Analysis and Machine Intelligence, 26*(7), 817-830.

Itti, L., & Koch, C. (2001). Computational Modelling of Visual Attention. *Nature Reviews Neuroscience, 2*(3), 194-203.

Itti, L., Koch, C., & Niebur, E. (1998). A Model of Saliency-Based Visual Attention for Rapid Scene Analysis. *IEEE Transactions on Pattern Analysis and Machine Intelligence, 20*(11), 1254-1259.

Kaufman, L., & Richards, W. (1969). Spontaneous Fixation Tendencies for Visual Forms. *Perception & Psychophysics, 5*(2), 85-88.

Kootstra, G., Nederveen, A., & De Boer, B. (2008, 1-4 September 2008). Paying Attention to Symmetry. In *proceedings of the British Machine Vision Conference*, Leeds, UK.

Le Meur, O., Le Callet, P., Barba, D., & Thoreau, D. (2006). A Coherent Computational Approach to Model Bottom-Up Visual Attention. *IEEE Transactions on Pattern Analysis and Machine Intelligence, 28*(5), 802-817.

Locher, P. J., & Nodine, C. F. (1987). Symmetry Catches the Eye. In J. K. O'Regan & A. Lévy-Schoen (Eds.), *Eye Movements: From Physiology to Cognition*. North-Holland: Elsevier Science Publishers B.V.

Olmos, A., & Kingdom, F. A. A. (2004). McGill Calibrated Colour Image Database, http://tabby.vision.mcgill.ca.

Ouerhani, N., von Wartburg, R., Hügli, H., & Müri, R. (2004). Empirical Validation of the Saliency-based Model of Visual Attention. *Electronic Letters on Computer Vision and Image Analysis, 3*(1), 13-14.

Palmer, S. E. (1991). Goodness, Gestalt, Groups, and Garner: Local Symmetry Subgroups as a Theory of Figural Goodness. In G. R. Lockhead & J. R. Pomerantz (Eds.), *The Perception of Structure. Essays in Honor of Wendell R. Garner* (pp. 23-40). Washington, DC: American Psychological Association.

Palmer, S. E., & Hemenway, K. (1978). Orientation and Symmetry: Effects of Multiple, Rotational, and Near Symmetries. *Journal of Experimental Psychology: Human Perception and Performance, 4*(4), 691-702.

Parkhurst, D. J., Law, K., & Niebur, E. (2002). Modeling the Role of Salience in the Allocation of Overt Visual Attention. *Vision Research, 42*, 107-123.

Parkhurst, D. J., & Niebur, E. (2003). Scene Content Selected by Active Vision. *Spatial Vision, 16*(2), 125-154.

Privitera, C. M., & Stark, L. W. (2000). Algorithms for Defining Visual Regions-of-Interest: Comparison with Eye Fixations. *IEEE Transactions on Pattern Analysis and Machine Intelligence, 22*(9), 970-982.

Reisfeld, D., Wolfson, H., & Yeshurun, Y. (1995). Context-Free Attentional Operators: The Generalized Symmetry Transform. *International Journal of Computer Vision, 14*, 119-130.

Richards, W., & Kaufman, L. (1969). "Center-of-Gravity" Tendencies for Fixations and Flow Patterns. *Perception & Psychophysics, 5*(2), 81-84.

Royer, F. L. (1981). Detection of Symmetry. *Journal of Experimental Psychology: Human Perception and Performance, 7*(6), 1186-1210.

Treisman, A. M., & Gelade, G. (1980). A Feature-Integration Theory of Attention. *Cognitive Psychology, 12*(1), 97-136.

Tyler, C. W. (2000). The Human Expression of Symmetry: Art and Neuroscience. In *proceedings of the ICUS Symmetry Symposium*, Seoul.